International Immunopharmacology 69 (2019) 217–224

Contents lists available at ScienceDirect

International Immunopharmacology

journal homepage: www.elsevier.com/locate/intimp

Generation and characterization of a specific single-chain antibody against DSPP as a prostate cancer biomarker: Involvement of bioinformatics-based design of novel epitopes

Seyed Nooreddin Faraji[a,c], Foroogh Nejatollahi[b,c,*], Ali-Mohammad Tamaddon[d], Mozafar Mohammadi[a], Ali Reza Aminsharifi[e]

[a] School of Advanced Medical Sciences and Technologies, Shiraz University of Medical Sciences, Shiraz, Iran
[b] Shiraz HIV/AIDS Research Center, Institute of Health, Shiraz University of Medical Sciences, Shiraz, Iran
[c] Recombinant Antibody Laboratory, Department of Immunology, Shiraz University of Medical Sciences, Shiraz, Iran
[d] Department of Nanotechnology, School of Pharmacy, Shiraz University of Medical Sciences, Shiraz, Iran
[e] Department of Urology, School of Medicine, Shiraz University of Medical Sciences, Shiraz, Iran

ARTICLE INFO

Keywords:
Dentin sialophosphoprotein (DSPP)
Epitope design
Single chain antibody (scFv)
Prostate cancer (PCa)
Molecular docking

ABSTRACT

Isolation of specific single chain antibodies (scFvs) against key epitopes of cancer markers are applied for cancer immunotherapy and diagnosis. In this study following the prediction of the 3D structure of the DSP part of Dentin sialophosphoprotein (DSPP), the epitope was chosen using in silico programs. Panning process was applied to isolate specific human scFv against the epitope. PCR and DNA fingerprinting differentiated the specific clones, which were evaluated by phage ELISA. Following DNA sequencing, the 3D structure of isolated scFv was modeled and Docked on DSP. Results demonstrated the selection of a specific anti-DSPP scFv with 40% frequency, which reacted significantly with the predicted epitope and PCa patients' urines in ELISA tests (P-value < 0.05). The VH and VL of the isolated scFv were from VH1 and VL3 gene families with several amino acid changes in CDRs and FRs domains. The scFv tightly bound to the DSP epitope with the lowest energy level by hydrogen bonds, cation-pi, hydrophobic and ionic interactions demonstrating the specificity of Ag-Ab interactions. The anti-DSPP scFv selected in this study with significant specificity to DSPP antigen offers a promising new agent for both PCa early detection and treatment of cancers with DSPP expression.

1. Introduction

Prostate cancer (PCa) is the second leading cause of cancer related death in men [1]. There are several confirmed risk factors for PCa including age, race, and positive family history. PCa incidence increases with age, and because of the increasing elderly population, the PCa prevalence had risen over the last decades. Development of effective early diagnostic strategies may decrease the mortality rate of PCa [2]. One of the main current diagnosis methods of PCa is trans-rectal ultrasound (TRUS) prostate biopsy. The criteria for men to undergo TRUS biopsy include prostate-specific antigen (PSA) serum levels and digital rectal examination (DRE). DRE is a subjective method and depends on the physicians' experience. Invasive biopsies fail to detect 10–30% of PCa [3]. Investigating other alternative or simultaneous ways along with TRUS biopsy, had no significant difference in diagnostic capacity of PCa [3,4].

On the other hand, many factors can affect PSA levels. PSA measures have great false positive results so that fewer than 30% of false positives will be biopsy positive for PCa. There is also a lack of correlation between PSA and PCa grading and staging [5].

Identifying novel serum markers specific to PCa not only has the potential to detect PCa in early stages and monitor disease progression but also might be useful for PCa targeting. Dentin sialophosphoprotein (DSPP) has been introduced as a proper target for PCa detection as its expression is very low in normal tissues. It also has a sensitivity of 90%, and a specificity of 100% for PCa confirmed by serum competitive ELISA. The mean value of DSPP is six folds in PCa sera compared to age-matched healthy individuals [6]. Also, the positive correlation between DSPP expression and pathological stage and aggressiveness of PCa has been revealed [7]. DSPP appears to be a reliable biomarker for PCa detection based on serum assays. Human DSPP gene codes a highly phosphorylated protein [8] that soon after expression, breaks to dentin

* Corresponding author at: Shiraz HIV/AIDS Research Center, Institute of Health, Shiraz University of Medical Sciences, Shiraz, Iran.
E-mail address: nejatollaf@sums.ac.ir (F. Nejatollahi).

https://doi.org/10.1016/j.intimp.2019.01.016
Received 17 November 2018; Received in revised form 10 January 2019; Accepted 10 January 2019
Available online 06 February 2019

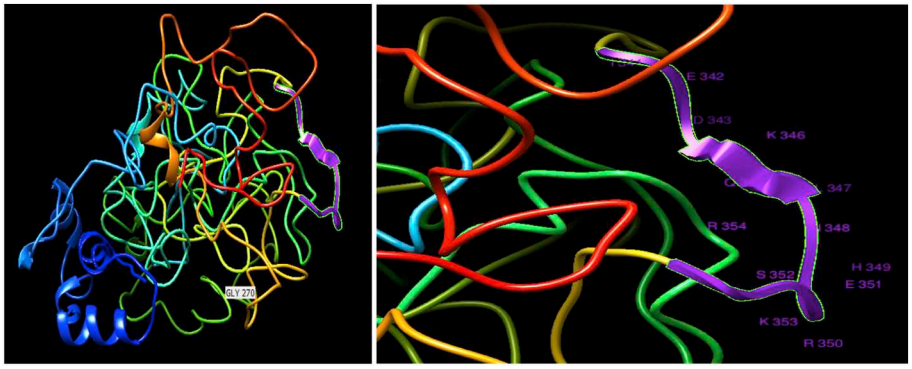

Fig. 1. 3D structure of human DSP using Modeler software (left). The selected peptide which is an accessible part of the molecule is shown in green shine, purple color and edged ribbon type. Focused presentation of DSP accessible epitope (14 amino acid residues) with 1-letter code + specifier (right).

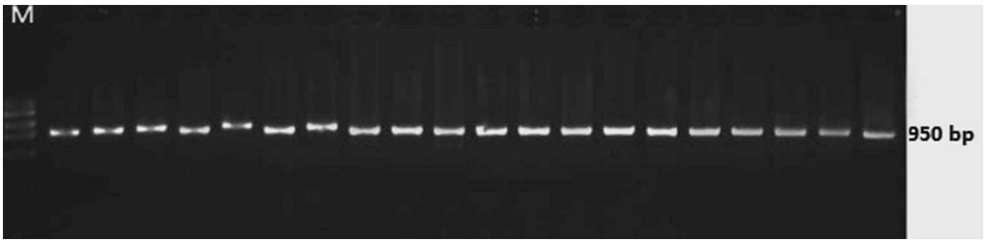

Fig. 2. PCR results of 20 randomly selected clones after panning. M is X174 DNA Marker.

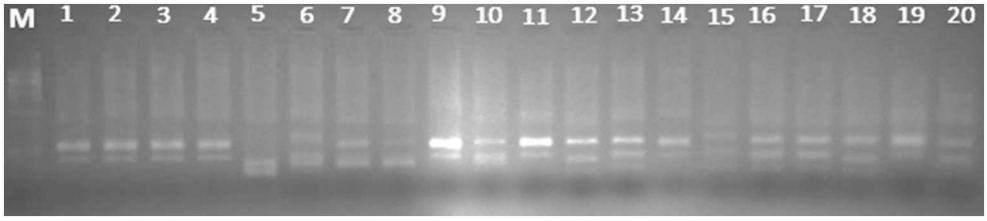

Fig. 3. DNA fingerprinting of the selected clones after panning. A dominant pattern is represented in lanes 1, 2, 3, 4, 9, 11, 14 and 19. M is X174 DNA Marker.

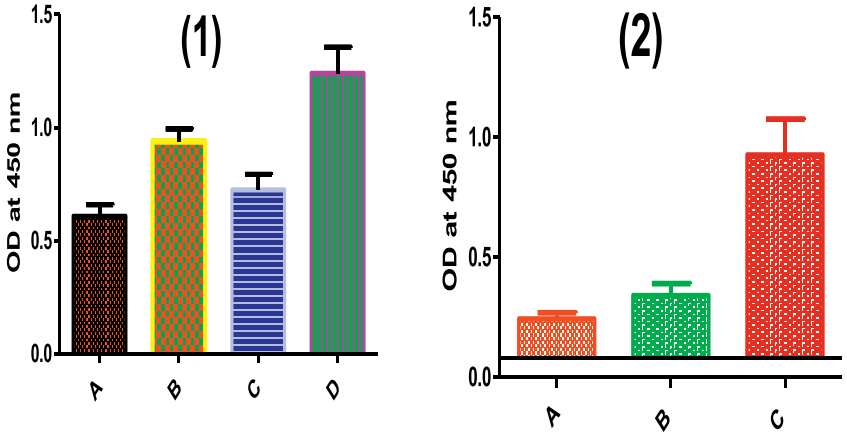

Fig. 4. (1) Phage-ELISA on designed epitope. The average absorbance (OD) of the reaction of specific anti-DSPP scFv (IR96 scFv) with no peptide well (A), unrelated scFv phage (B), unrelated peptide (C) and DSP peptide (D). (2) Phage-ELISA on PCa patient's urine. The average absorbance (OD) of the reaction of specific anti-DSPP scFv (IR96 scFv) with no antigen well (A), healthy individuals' urines (B) and PCa patients' urines (C).

sialoprotein (DSP) and dentin phosphoprotein (DPP) so that the amount of whole DSPP in the extracellular matrix (ECM) of dentin is less than DSP or DPP parts and is hardly detectable. No 3D structure has been reported for DSPP in protein databases. DPP part of DSPP contains over 200 tandem repeats of serine aspartate (SSD) and facilitates the maturation of dentin. However, its function is not yet fully understood [9].

Several monoclonal antibodies (mAbs) have been employed for DSPP targeting. However clinical application of mAbs have some limitations including prolonged circulating half-life, complex structures, relatively large molecular sizes, susceptibility to physical instability, tend to aggregation and high costs of production [10,11]. Single-chain variable fragment (scFv) Abs are one of the most popular recombinant antibody (rAb) format and an alternative to full-length monoclonal antibodies in both diagnostic and therapeutic purposes. Up to now, a significant number of scFvs are selected against cancer cell markers, and their effects have been reported [12]. ScFvs are composed of variable heavy (VH) and variable light (VL) chains that are assembled by a peptide linker. These small antibodies could create the complete antigen-binding site of an antibody molecule [13]. The benefits of scFv include wholly human in origin thus the human anti-mouse antibody

IR96 scFv, VH chain

Region	VH- FR1																												VH- CDR 1						
VH1 gene family	E	V	Q	L	Q	Q	S	G	A	E	L	V	R	S	G	A	S	V	K	L	S	C	T	A	S	G	F	N	I	K	D	Y
IR96 scFv	R	G	A	A	G	G	V	W	T	E	L	V	R	S	G	A	S	V	K	L	S	C	T	A	S	G	F	N	I	K	D	Y
Numbering	H1	H2	H3	H4	H5	H6	H7	H8	H9	H10	H11	H12	H13	H14	H15	H16	H17	H18	H19	H20	H21	H22	H23	H24	H25	H26	H27	H28	H29	H30	H31	H32

Region	VH- FR2																	VH- CDR 2					VH- FR3						
VH1 gene family	Y	M	H	W	V	K	Q	R	P	E	Q	G	L	E	W	I	G	W	I	D	-	E	N	G	D	T	E	Y	A	P	K
IR96 scFv	Y	M	H	W	V	K	Q	R	P	E	Q	G	L	E	W	I	G	W	I	E	P	E	N	G	D	T	E	Y	A	P	K
Numbering	H33	H34	H35	H36	H37	H38	H39	H40	H41	H42	H43	H44	H45	H46	H47	H48	H49	H50	H51	H52	H52A	H53	H54	H55	H56	H57	H58	H59	H60	H61	H62

Region	VH- FR3																														
VH1 gene family	F	Q	G	K	A	T	M	T	A	D	T	S	S	N	T	A	Y	L	Q	L	-	-	-	T	S	E	D	T	A	V	Y
IR96 scFv	S	Q	G	K	A	T	M	T	A	D	T	S	S	N	T	A	Y	L	Q	L	S	S	L	T	S	E	D	T	A	V	Y
Numbering	H63	H64	H65	H66	H67	H68	H69	H70	H71	H72	H73	H74	H75	H76	H77	H78	H79	H80	H81	H82	H82A	H82B	H82C	H83	H84	H85	H86	H87	H88	H89	H90

Region	VH- FR3				VH- CDR 3								VH- FR4										
VH1 gene family	Y	C	N	A	D	G	N	S	W	F	A	Y	W	G	Q	G	T	L	V	T	V	S	A
IR96 scFv	Y	C	N	A	D	G	N	Y	W	F	A	Y	W	G	Q	G	T	M	V	T	V	S	S
Numbering	H91	H92	H93	H94	H95	H96	H97	H98	H99	H100	H101	H102	H103	H104	H105	H106	H107	H108	H109	H110	H111	H112	H113

Fig. 5. VH amino acid changes of IR96 scFv compared to VH1 germ line gene family based on AbYsis and Vbase2 servers: White color: No change, Red color: change to the unusual residue, Yellow color: change to the usual residue and Green color: insertion. Unusual residues are amino acids with < 1% frequency of a sequence.

Region	VL- FR1																						VL- CDR 1						
VL3 gene family	S	S	E	L	T	Q	D	P	A	...	V	S	V	A	L	G	Q	T	V	R	I	T	C	Q	G	D	S	L	R	S
IR96 scFv	S	Y	V	L	T	Q	D	P	A	...	A	S	V	A	L	G	Q	T	V	R	I	T	C	Q	G	D	S	L	R	S
Numbering	L1	L2	L3	L4	L5	L6	L7	L8	L9	L10	L11	L12	L13	L14	L15	L16	L17	L18	L19	L20	L21	L22	L23	L24	L25	L26	L27	L28	L29	L30

Region	VL- CDR 1					VL- FR2												VL- CDR 2						VL- FR3						
VL3 gene family	Y	Y	A	S	W	Y	Q	Q	K	P	G	Q	A	P	V	L	V	I	Y	G	K	N	N	R	P	S	G	I	P	D	R	F
IR96 scFv	Y	Y	V	S	W	F	Q	Q	K	P	G	Q	A	P	V	F	V	M	Y	G	Q	N	N	R	P	S	G	I	P	D	R	F
Numbering	L31	L32	L33	L34	L35	L36	L37	L38	L39	L40	L41	L42	L43	L44	L45	L46	L47	L48	L49	L50	L51	L52	L53	L54	L55	L56	L57	L58	L59	L60	L61	L62

Region	VL- FR3																									VL- CDR 3					
VL3 gene family	S	G	S	S	S	G	N	T	A	S	L	T	I	T	G	A	Q	A	E	D	E	A	D	Y	Y	C	N	S	R	D	S	S
IR96 scFv	S	G	S	S	S	G	N	T	A	S	L	T	I	T	G	A	Q	A	E	D	E	A	D	Y	Y	C	H	S	R	D	S	S
Numbering	L63	L64	L65	L66	L67	L68	L69	L70	L71	L72	L73	L74	L75	L76	L77	L78	L79	L80	L81	L82	L83	L84	L85	L86	L87	L88	L89	L90	L91	L92	L93	L94

Region	VL- CDR 3						VL- FR4												
VL3 gene family	G	-	-	-	R	V	F	G	G	G	T	K	L	T	V	-	G	A	A
IR96 scFv	G	T	H	L	R	V	F	G	G	G	T	K	V	T	V	L	G	A	A
Numbering	L95	L95A	L95B	L95C	L96	L97	L98	L99	L100	L101	L102	L103	L104	L105	L106	L106A	L107	L108	L109

Fig. 6. VL amino acid changes of IR96 scFv compared to VL3 germ line gene family based on AbYsis and Vbase2 servers: White color: No change, Red color: change to the unusual residue, Yellow color: change to the usual residue and Green color: Insertion. Unusual residues are amino acids with < 1% frequency of a sequence.

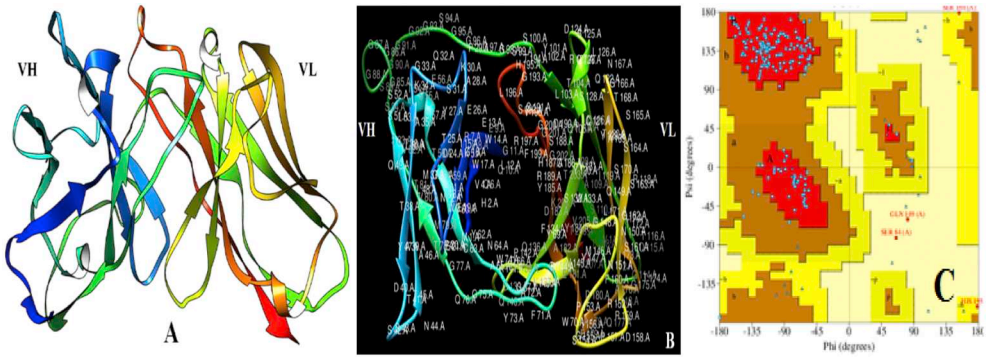

Fig. 7. The 3D structure of IR96 scFv obtained from homology modeling. Rounded ribbon style created by Chimera shows domains and second structures of the molecule by different colors (A). The top view of the same fragment with names and numbers of residues (B). Ramachandran plot of the modeled IR96 scFv (C).

response (HAMA) doesn't induce, improved pharmacokinetic properties, lacking the Fc region and subsequently lower immunogenicity, lower retention times in non-target tissues, high affinity and a small size (26–27 kDa) that permits reaching to cryptic epitopes which are not accessible to full-sized mAbs [14–16].

In the present study, the 3D structure of DSPP was predicted using ab initio bioinformatics tools. The best antigenic and accessible epitope was selected using in silico techniques. Following selection of anti-DSPP scFv antibody by panning procedure and evaluation of specificity of the selected scFv using phage-ELISA, sequence analysis of specific anti-DSPP scFv was performed to determine the amino acid specific changes in the anti-DSPP scFv. The docking of anti-DSPP scFv with DSPP antigen was done to investigate the antigen-antibody interactions and determinate the most important amino acids in the interaction.

2. Materials and methods

2.1. DSPP epitope prediction and evaluation

The three dimensional (3D) structure of DSP part of DSPP protein was predicted by Quark ab initio protein structure prediction server and modeler, version 9.11 [17,18]. For visualizing the 3D structures of

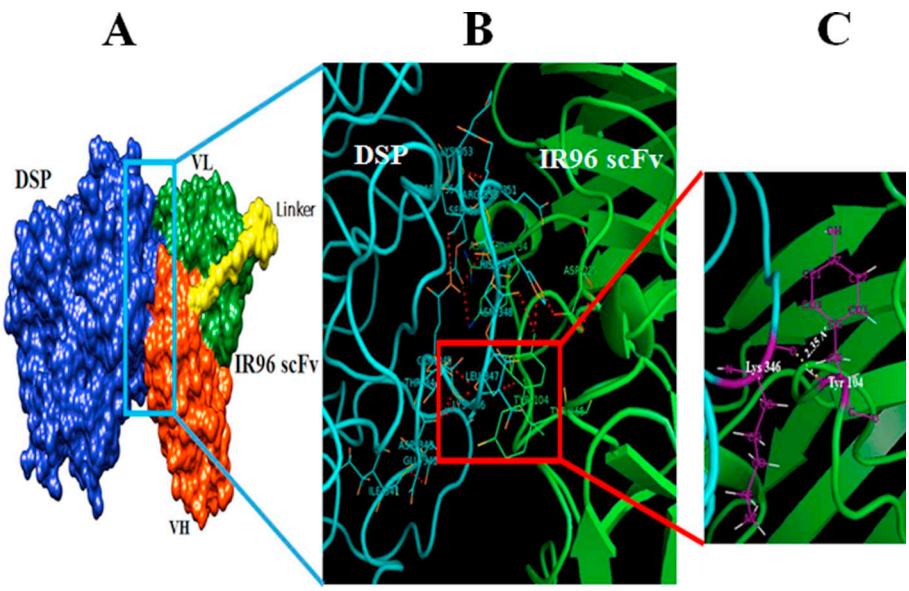

Fig. 8. Docking of the IR96 scFv with DSP antigen according to ZDOCK server. Visualizations were performed in PyMOL software. DSP is shown in blue color. VH, VL, and linker of IR96 scFv are shown in green, orange and yellow color, respectively (A). Focused presentation of anti-DSPP scFv and DSP epitope and important residues in Ag-Ab interactions (B) and the hydrogen bond interaction between Tyr 104 from VHCDR3 of IR96scFv with Lys 346 from DSP epitope (C).

protein, structure refinements and energy minimization, Chimera 1.10.2 software and ModRefiner at https://zhanglab.ccmb.med.umich.edu/ModRefiner/ were applied [19]. The IEDB analysis resource server at http://tools.iedb.org/main/bcell/ and SVMTriP program at http://sysbio.unl.edu/SVMTriP/ were applied for prediction of a linear accessible and antigenic epitope on DSPP antigen.

2.2. Phage rescue

A phage antibody display library of scFv was produced as previously described [20,21]. To rescue the library, *Escherichia coli* TG1 bacteria containing phagemid were cultured overnight on 2TY agar containing 1% glucose and 100 μg/ml ampicillin (2TYG/amp) at 30 °C. The bacteria were scraped and incubated in 2TYG broth at 37 °C for 1 h. M13KO7 helper phage (New England Biolabs, UK) was added and incubated at 37 °C for 1 h with shaking. The culture was centrifuged, and the bacterial pellet was transferred to a 2TY broth containing ampicillin (100 μg/ml) and kanamycin (50 μg/ml) and incubated with constant shaking at 30 °C overnight. The culture was centrifuged at 5500 rpm for 30 min and the supernatant containing phage-scFvs filtered through sterile 0.45 μm filters.

2.3. Panning procedure

Following epitope design, the DSP peptide with > 85% purity was synthesized by TAG Copenhagen Company (Denmark). Nunc immunotube (Nunc, Denmark) was coated with the peptide at 10 μg/ml concentration and incubated overnight at 4 °C. Immunotube was washed with PBS and coated with 2% skimmed milk solution as a blocking solution. The immunotube was washed with PBS, and $\sim 10^{12}$ phage library diluted 1:1 with the blocking solution was added and incubated for 1 h. Following washing the tubes with PBS-0.05% Tween^{20} (PBST) and PBS, logarithmic phase TG1 cells were added and incubated for 1 h at 37 °C. The TG1 cells infected by phage-scFvs was collected using centrifugation. Four rounds of selections were performed to select specific scFv antibodies against the DSPP epitope. After each round of panning, phage precipitation using PEG/NaCL, phage titration, PCR and DNA fingerprint was performed to control the test progress.

2.4. Phage particle titration and precipitation

For determination of phage concentration of each rescued phage, 10 μl of phage antibody supernatant was added to 1 ml of log phase TG1 *E. coli* and incubated with shaking at 37 °C for 1 h. Serial dilution of bacteria was prepared and cultured on to 2TY Agar/Ampicillin medium for overnight at 30 °C. The number of clones per dilution was determined, and phage concentration titer per milliliter was calculated. Rescued phages were concentrated according to standard PEG/NaCl precipitation method. Briefly, 40 ml 0f the phage supernatant was mixed with 10 ml of 20% polyethylene glycol (PEG)/2.5% NaCl and placed on ice for 1 h and centrifuged in 4 °C for 15 min at 10,000 rpm. Following centrifugation, the pellet was resuspended in PBS and centrifuged at 13,000 rpm for 2 min to remove any residual bacterial cell debris. For each subsequent panning step, a titer of $\sim 10^{12}$ amplified phage particles of the previous enrichment round was used.

2.5. PCR and DNA fingerprinting of the selected clones against DSPP

To determine the common patterns with high frequency, PCR and DNA fingerprinting of 20 randomly selected clones from the 4th round of panning was performed. The clones were picked off from the culture plate, heated at 94 °C to lyse the bacteria and PCR was performed using vector primers. The PCR program was as follows: denaturation 1 min at 94 °C, annealing 1 min at 55 °C and elongation time 2 min at 72 °C. PCR products were digested by Mva-1 restriction endonuclease at 37 °C for 2 h. The digested products were run on 2.5% agarose gel.

2.6. Enzyme-linked immunosorbent assay

Phage-ELISA was performed on both the designed DSP epitope and PCa patient's urine containing DSPP antigen. Plates (Nunc, Denmark) were coated with 5 μg of DSP peptide and incubated overnight at 4 °C. Unrelated peptide, unrelated scFv phage (scFv phage against HER2) and no peptide wells were also considered as negative controls. To evaluate the isolated scFv against PCa patient's urine, 100 μl of PCa patient's urine (n = 10) were applied. Healthy individuals' urine (n = 10) and no antigen well were used as negative controls. The experiments were performed in triplicate. The plates were blocked with 2% skimmed milk for 2 h at 37 °C. After washing with PBS, anti-DSPP displaying phages were added to the wells and incubated at RT for 2 h. Following washing with PBST and PBS, rabbit anti-fd bacteriophage antibody was added and incubated 1.5 h at 37 °C. The plates were washed three times with PBST and three times with PBS. Afterward, HRP-conjugated anti-rabbit antibody (Sigma, UK) was added and incubated 1 h at RT. The plates were washed with PBS, and bounded phages were detected by TMB substrate and H_2SO_4 as a stop solution.

Table 1
Hydrogen bonds interaction of IR96 scFv and DSPP antigen.

Type of interaction	Antibody (scFv)			Antigen (DSP)		Distance
	Location	Residue	Atom	Residue	Atom	
Hydrogen bond (main chain-main chain)	VH-CDR3	Tyr 104	N	Lys 346	O	2.35
Hydrogen bond (main chain-side chain)	VH-CDR3	Tyr 104	OH	His 349	ND1	2.28
	VH-CDR3	Tyr 104	OH	His 349	ND1	2.28
	VL-CDR3	Asp 225	OD1	His 349	NE2	1.98
	VL-CDR3	Asp 225	OD1	His 349	NE2	1.98
	VL-CDR3	Asp 225	OD1	His 349	NE2	1.98
	VH-CDR1	Tyr 34	OH	Arg 354	NH1	2.79
	VH-CDR1	Tyr 34	OH	Arg 354	NH1	2.79
	VH-FR2	Trp 52	NE1	Glu 351	OE2	3.43
	VL-CDR1	Try 165	OH	Glu 241	OE1	2.95
	VL-CDR3	Arg 232	NH1	Glu 351	OE1	3.05
	VL-CDR3	Arg 232	NH1	Glu 351	OE1	3.05
Hydrogen bond (side chain-side chain)	VH-CDR3	Tyr 104	OH	Leu 347	O	2.79
	VH-CDR3	Tyr 104	OH	Asn 348	O	2.86
	VH-CDR3	Gly 102	O	Asn 348	OD1	3.01
	VH-CDR3	Gly 102	O	Asn 348	OD1	3.01
	VL-CDR3	Arg 224	O	His 349	ND1	3.48
	VH-FR1	Tyr 35	OH	Lys 353	N	2.71
	VH-FR2	Tyr 35	OH	Glu 351	O	2.16
	VH-CDR2	Asp 33	O	Arg 354	NE	2.27
	VH-CDR1	Asp 33	O	Arg 354	NH1	2.70
	VH-CDR1	Asp 33	O	Arg 354	NH1	2.70
	VH-CDR2	Glu 56	OE2	Gly 442	N	2.78

Red color represents IR96 scFv antibody and green color represents DSP antigen.

The absorbance was measured by ELISA reader at 450 nm, and the average OD was calculated. Informed consent was used for each person prior to the study when the patients' urines were used.

2.7. Plasmid extraction and sequencing of the isolated scFv

The plasmid of the selected clone was extracted with alkaline lysis method. Cells from bacterial culture were harvested by centrifugation and resuspended in 50 mM Tris buffer, pH 8.0, containing 10 mM EDTA. The suspension was treated with an equal volume of cell lysis buffer containing 0.2 M NaOH and 1% SDS, followed by an equal volume of neutralizing solution (3 M potassium acetate, pH 5.0). Precipitated material was removed by centrifugation and transparent supernatant containing plasmid DNA was concentrated by ethanol precipitation method. The extracted plasmids were quantitated using Nano drop spectrophotometer (Thermo Scientific, USA). To determine the nucleic acid sequence of the isolated scFv, PCR with pfu DNA polymerase was done on both PCR products and extracted plasmids. The anti-DSPP scFv was sequenced using the Sanger sequencing method. Amino acid sequence alignments of the isolated scFv with VH/VL germ line gene families were done using the VBASE2 and AbYsis servers (http://www2.mrc-lmb.cam.ac.uk/vbase/alignments2.php and http://www.bioinf.org.uk/abysis2.7/).

2.8. Homology modeling of anti-DSPP scFv and docking against predicted DSPP

The 3D structure of anti-DSPP scFv, IR96 scFv, was created using SWISS-MODEL server [22–24]. To evaluate the stereochemical quality of the predicted structure, PROCHECK software was used. The interactions between predicted DSPP and modeled scFv antibody were analyzed using ZDOCK server at http://zdock.umassmed.edu. To obtain better results and limiting wide interactions, advanced options such as masking non- complementary determining regions (non-CDRs) was performed. Among queries, best docking result with the lowest energy level was selected and further evaluations on antigen-antibody interaction forces were done using protein interactions calculator (PIC) at http://pic.mbu.iisc.ernet.in/.

2.9. Statistical analysis

Statistical analysis on phage-ELISA results was performed using One-way ANOVA. Data are presented as the mean ± standard deviation. P values of < 0.05 were considered statistically significant.

3. Results

3.1. Prediction of DSPP epitope

To select an immunodominant epitope from DSPP antigen, among the output sequences results of IEDB and SVMTriP servers, based upon criteria such as accessibility and antigenicity, a 14 amino acid sequence (IEDTQKLNHRESKR) was selected for further experiments. The peptide was selected from amino acid 341–355 of the DSP protein. Prediction of linear epitopes from both servers based on surface accessibility showed that the HRESKR amino acid sequence part of the peptide had the highest score (3.409) among 450 suggested peptides. Also, the antigenicity of the selected peptide was near maximum score (0.996). The predicted 3D structure of DSP with the selected peptide is shown in Fig. 1.

3.2. PCR and DNA fingerprinting of the selected clones

PCR results of 20 randomly clones after four rounds of panning represented 950 bp bonds related to scFv gene inserts (Fig. 2). DNA fingerprinting of the PCR products showed a dominant pattern with frequency of 40% (8 out of 20 patterns) (Fig. 3).

Table 2
Cation-Pi interaction of IR96 scFv and DSPP antigen.

Type of interaction	Antibody (scFv)		Antigen (DSP)	Distance
Cation-Pi	Location	Residue	Residue	
	VH-CDR1	Tyr 34	Arg 354	3.94
	VH-CDR3	Phe 106	Lys 346	3.93

Red color represents IR96 scFv antibody and green color represents DSP antigen.

3.3. Phage ELISA

To evaluate the affinity of the selected anti-DSPP displaying phage, IR96 scFv, to the corresponding epitope and DSPP antigen secreted in PCa patients´ urines, the phage ELISA procedure was done. The IR96 scFv demonstrated significant ELISA binding capacity to both peptide epitope and DSP antigen. As shown in Fig. 4-1, at OD 450 nm, the mean absorbance of the reaction of IR96 scFv to the corresponding peptide was 1.24 while the mean absorbance of the reaction of the antibody to no peptide, unrelated phage and unrelated peptide wells were 0.6, 0.8 and 0.7, respectively (P value < 0.05). In Fig. 4-2, the mean absorbance of the reaction of IR96 scFv to the corresponding DSPP in PCa patients' urines was 0.92 while the mean absorbance of the reaction of the antibody to healthy individual' urines and no antigen wells were 0.34 and 0.24, respectively (P value < 0.05).

3.4. IR96 scFv sequence analysis

Sequence analysis of IR96 scFv in Vbase2 and AbYsis servers showed that VH and VL are from VH1 and VL3 gene family, respectively. There were some amino acid (AA) changes in CDRs and FRs of the both VH and VL chains of IR96 scFv compared to VH1/VL3 gene families. VH had 4 amino acid insertions, and 15 amino acid substitutions containing substitutions to usual or unusual residues (Fig. 5) and VL had 4 AA insertions and 10 amino acid substitutions to usual or unusual residues (Fig. 6). The accession number assigned for IR96 scFv nucleotide sequence in GenBank is KX531000 reachable at https://www.ncbi.nlm.nih.gov/nuccore/KX531000. The IR96 scFv full-length sequence is as follows:

HGRGAAGGVWTELVRSGASVKLSCTASGFNIKDYYMHWVKQRPEQGLEWIGWIEPENGDTEYAPKSQGKATMTADTSSNTAYLQLSSLTSEDTAVYYCNADGNYWFAYWGQGTMVTVSSGGGGSGGGGSGGGGSSYVLTQDPAASVALGQTVRITCQGDSLRSYYVSWFQQKPGQAPVFVMYGQNNRPSGIPDRFSGSSSGNTASLTITGAQAEDEADYYCHSRDSSGTHLRVFGGGTKVTVLGAA. Where the VH sequence is HGRGAAGGVW…(99^{aa})…GQGTMVTVSS, linker is GGGGSGGGGSGGGGS and VL sequence is SYVLTQDPAA…(92^{aa})…GTKVTVLGAA.

3.5. Homology modeling and evaluation of the modeled scFv

The protein sequence of the IR96 scFv was rendered to the SWISS-MODEL server and the most homologous protein, 1qok. 1. A was selected for modeling. The IR96 scFv had 72% identity and 98% coverage with this scFv. Further evaluations were done on predicted 3D structure of IR96 scFv (Fig. 7-A and B). Following structure refinement, Ramachandran plot assessment by RAMPAGE showed that 96.5% of residues located in the most favored regions. Also, total G-Factor was −0.22 (Fig. 7-C).

3.6. Docking of isolated anti-DSP scFv with predicted DSP

The best docking result of IR96 scFv and DSP performed by ZDOCK server was selected which had the lowest energy score of −310.8 Kcal/mol. Evaluation of the two molecules orientation to one another using PyMol, showed that 14 amino acids are involved in the interactions between IR96 scFv and DSP epitope (Fig. 8). Tables 1–4 represent the different interactions between antigen and antibody including hydrogen bonds (between main chain or side chain of an amino acid residue in antibody molecule with a main chain or side chain of an amino acid residue in antigen molecule), cation-pi, hydrophobic and ionic interactions.

4. Discussion

The specificity and sensitivity of current reference standard biomarkers for PCa diagnosis are controversial. Many alternative secretory protein biomarkers have been suggested for PCa diagnosis instead of PSA including urinary PCA3 and TMPRSS2-ERG fusion [25]. However, they have variable sensitivity and specificity, and their expression profile doesn't change in different stages of PCa [26]. Among reported biomarkers, DSPP has emerged as a potentially valuable biomarker not only for early detection of PCa but also for PCa targeting [6]. This study is the first report representing a specific anti-DSPP scFv for targeting the DSPP antigen toward PCa diagnosis and therapy. Since no description of 3D structure or a proper homologous protein for DSPP in protein data bank was found, we predicted DSPP 3D structure. Ab initio computational methods are appropriate tools to predict the accessible epitope of antigens [27,28]. In this study, only the DSP part of DSPP was applied for in silico analysis and the DPP part of the molecule was deleted because of its SSD repeat property. It has been reported that the majorities of antibodies against DSPP, target DSP part of this antigen [29]. To choose the accessible epitope of DSPP antigen for selection of specific anti-DSPP scFv in panning procedure, IEDB and SVMTriP tools were used. A linear immunodominant epitope with 14 residues (IEDTQKLNHRESKR) was selected among the presented sequences, according to accessibility and antigenicity properties. To determine any homology between the desired epitope sequence and other proteins, blasting of the selected peptide sequence against the protein reference sequences was performed on NCBI data bank. The DSP designed epitope showed no identity to the other proteins.

To select specific scFv against designed DSP, phage display technique and panning process were used. A specific scFv with 40%

Table 3
Hydrophobic interaction of IR96 scFv and DSPP antigen.

Type of interaction	Antibody (scFv)		Antigen (DSP)
Hydrophobic	Location	Residue	Residue
	VH-CDR3	Tyr 104	Leu 347
	VL-CDR1	Tyr 165	Leu 347

Red color represents IR96 scFv antibody and green color represents DSP antigen.

Table 4
Ionic interaction of IR96 scFv and DSPP antigen.

Type of interaction	Antibody (scFv)		Antigen (DSP)
Ionic	Location	Residue	Residue
	VH-CDR1	Asp 33	Arg 354
	VH-CDR2	His 37	Glu 351
	VL-CDR3	Arg 224	Glu 351
	VL-CDR3	Arg 232	Glu 351
	VL-CDR3	Asp 225	Glu 351

Red color represents IR96 scFv antibody and green color represents DSP antigen.

frequency was selected. Further examination by phage ELISA showed that the average absorbance of the wells coated with patients' urines containing DSPP was significantly higher than those of healthy individuals' urines and no antigen wells (OD: 0.92 versus 0.34 and 0.24, respectively). This represented the specificity of anti-DSPP scFv against DSPP antigen. The specificity of scFvs against some cancer targets including EGFR and CTLA-4 antigens are shown by phage-ELISA studies [30,31]. To find the molecular basis of IR96 scFv, the isolated scFv was sequenced. Sequence analysis of the IR96 scFv showed several amino acid (AA) changes in the both CDRs and FRs of VH and VL chains compared to germ line gene families, VH1 and VL3. Four AA insertions and 15 residue substitutions were found in VH domain, and 4 AA insertions and 10 residue substitutions were found in VL domain which represents the specificity of the antibody molecule. In HCDR3 sequence, serine (S) was substituted by tyrosine (Y). It has been reported that diversity in the HCDR3 plays a dominant role in antigen binding and a single AA change may seriously disrupt site structure and may abolish antigen binding [32,33]. Some AA changes in the frameworks of the VH domain of IR96 scFv were observed especially 8 constant AA changes in FR1. The critical role of FR1 in the antibody specificity is shown [34]. The role of other framework regions in the improvement of specificity and binding kinetics of antibody are also reported [35]. It was found that the number of overall AA changes in IR96 VH were more than VL which also confirmed the specific selection of IR96 antibody against DSPP. The importance of VH specificity in epitope binding has been described [32].

To show the importance of AA changes of isolated scFv on interaction with its antigen, molecular docking was run using ZDOCK server on the modeled IR96 scFv and DSP molecules. In silico docking prediction methods can reveal key determinants of antibody-antigen binding. Moreover, calculating the energy of interaction provides a prediction of the involvement of specific residues at the interaction interface [36]. The docking results showed that IR96 scFv tightly binds to the selected epitope of DSP molecule with the lowest energy level (−310.8 Kcal/mol). This energy lowering in the antibody-antigen (Ab-Ag) complex is mainly due to stabilizing by hydrogen bonding, salt bridges and hydrophobic interactions [37]. The specificity of the recognition was shown to originate principally from multiple Cation-Pi interactions (CH-π) and hydrogen bonds [38,39]. CH-π interaction which is a non-covalent molecular interaction between the face of an electron-rich π system (e.g., benzene) and an adjacent cation, has been reported as an essential factor which profoundly affects Ag-Ab interaction [39]. We further analyzed the CH-π interactions and the hydrogen bond between IR96 scFv and DSPP. Most frequent cation-π interactions within proteins occur by 5 residues including lys, arg, phe, tyr and trp. A 6.0-Å and 3 Å distance cutoff were used for cation-pi interactions and hydrogen bonds, respectively. In cation-pi interactions of IR96 scFv and DSP antigen, lys, arg, phe, and tyr amino acids participated. CDR3 residues of VH and VL of IR96 showed 56% (18/32) of all CDR interactions. There were several hydrogen bonds (n = 23) between DSP epitope and IR96 scFv including interactions of main chain and the side chain of amino acids in antibody molecule with the main chain and/or side chain amino acids of DSP. Our results showed that 3 tyrosine residues including Tyr 34, Tyr 35 and Tyr 104 of scFv participated in 13 out of 32 interactions (40%). Among these tyrosines, Tyr 104 of VHCDR3 involved in 46% (6/13) of interactions formed by tyrosines and about 18% of all CDR interactions. The vital role of interfacial tyrosine in antigen recognition was confirmed [40,41]. Critical residues of DSP epitope that participated in Ag-Ab interactions were Lys 346, Leu 347, His 349 and Arg 354. This AA composition of the epitope is in accordance with previous findings that conformational B cell epitopes are usually rich in charged and polar amino acids [42]. These results demonstrated the specificity of Ag-Ab interactions.

The specific anti-DSPP scFv selected in this study with significant specificity to DSPP antigen in both experimental and bioinformatic evaluations offers a promising new molecule for PCa early detection assay. Since DSPP is expressed in different cancers and its gene silencing inhibits key tumorigenic activities [43], the specific anti-DSPP scFv, IR96 scFv, may also be applied as a therapeutic agent for several cancers in which DSPP expression occurs. Recently, Wan et al. [44] revealed that DSP interacts with cell surface receptors and subsequently activates several intracellular signaling and regulates DSPP expression via a positive feedback loop. Therefore, blocking DSP by IR96 scFv may inhibit downstream activities and control DSPP expression. As the scFv antibodies can be genetically manipulated and form fusion proteins with additional effector function, the specific anti-DSPP selected in this study has the potential to be conjugated with other molecules to be more useful for clinical applications.

Acknowledgments

This article was extracted from Ph.D. thesis written by Seyed Nooreddin Faraji, grant No 94-7584 and financially supported by Shiraz University of Medical Sciences, Shiraz, Iran.

The authors declare no competing interests.

References

[1] A.C. Groner, L. Cato, J. de Tribolet-Hardy, T. Bernasocchi, H. Janouskova, D. Melchers, et al., TRIM24 is an oncogenic transcriptional activator in prostate Cancer, Cancer Cell 29 (6) (2016) 846–858.
[2] M.F. Leitzmann, S. Rohrmann, Risk factors for the onset of prostatic cancer: age, location, and behavioral correlates, Clin. Epidemiol. 4 (2012) 1–11.
[3] A.P. Astrand, B.M. Andersson, V. Jalkanen, B. Ljungberg, A. Bergh, O.A. Lindahl, Prostate cancer detection with a tactile resonance sensor-measurement considerations and clinical setup, Sensors (Basel, Switzerland). 17 (11) (2017).
[4] Y. Tang, Z. Liu, L. Tang, R. Zhang, Y. Lu, J. Liang, et al., Significance of MRI/transrectal ultrasound fusion three-dimensional model-guided, targeted biopsy based on transrectal ultrasound-guided systematic biopsy in prostate cancer detection: a systematic review and meta-analysis, Urol. Int. 100 (1) (2018) 57–65.
[5] M. Cortesi, E. Fridman, A. Volkov, S. Shilstein, R. Chechik, A. Breskin, et al., New prospective for non-invasive detection, grading, size evaluation, and tumor location of prostate cancer, Prostate 70 (15) (2010) 1701–1708.
[6] A. Jain, D.A. McKnight, L.W. Fisher, E.B. Humphreys, L.A. Mangold, A.W. Partin, et al., Small integrin-binding proteins as serum markers for prostate cancer detection, Clin. Cancer Res. 15 (16) (2009) 5199–5207.
[7] M. Chaplet, D. Waltregny, C. Detry, L.W. Fisher, V. Castronovo, A. Bellahcene, Expression of dentin sialophosphoprotein in human prostate cancer and its correlation with tumor aggressiveness, Int. J. Cancer - Journal international du cancer. 118 (4) (2006) 850–856.
[8] S. Suzuki, N. Haruyama, F. Nishimura, A.B. Kulkarni, Dentin sialophosphoprotein and dentin matrix protein-1: two highly phosphorylated proteins in mineralized tissues, Arch. Oral Biol. 57 (9) (2012) 1165–1175.

[9] Y. Sun, S. Ma, J. Zhou, A.K. Yamoah, J.Q. Feng, R.J. Hinton, et al., Distribution of small integrin-binding ligand, N-linked glycoproteins (SIBLING) in the articular cartilage of the rat femoral head, J. Histochem. Cytochem. Off. J. Histochem. Soc. 58 (11) (2010) 1033–1043.
[10] C.H. van Dyck, Anti-amyloid-beta monoclonal antibodies for Alzheimer's disease: pitfalls and promise, Biol. Psychiatry 83 (4) (2018) 311–319.
[11] H. Kobayashi, P.L. Choyke, M. Ogawa, Monoclonal antibody-based optical molecular imaging probes; considerations and caveats in chemistry, biology and pharmacology, Curr. Opin. Chem. Biol. 33 (2016) 32–38.
[12] N.E. Weisser, J.C. Hall, Applications of single-chain variable fragment antibodies in therapeutics and diagnostics, Biotechnol. Adv. 27 (4) (2009) 502–520.
[13] M. Mohammadi, F. Nejatollahi, Y. Ghasemi, S.N. Faraji, Anti-metastatic and anti-invasion effects of a specific anti-MUC18 scFv antibody on breast cancer cells, Appl. Biochem. Biotechnol. 181 (1) (2017) 379–390.
[14] B. Moazen, E. Ebrahimi, F. Nejatollahi, Single chain antibodies against gp55 of human cytomegalovirus (HCMV) for prophylaxis and treatment of HCMV infections, Jundishapur J. Microbiol. 9 (3) (2016) e16241.
[15] B. Ehsaei, F. Nejatollahi, M. Mohammadi, Specific single chain antibodies against a neuronal growth inhibitor receptor, nogo receptor 1: promising new antibodies for the immunotherapy of multiple sclerosis, Shiraz E-Med. J. 18 (1) (2017) 453–458.
[16] F. Nejatollahi, P. Bayat, B. Moazen, Cell growth inhibition and apoptotic effects of a specific anti-RTFscFv antibody on prostate cancer, but not glioblastoma, cells, F1000Research. 6 (2017) 156.
[17] D. Xu, Y. Zhang, Ab initio protein structure assembly using continuous structure fragments and optimized knowledge-based force field, Proteins 80 (7) (2012) 1715–1735.
[18] A. Sali, T.L. Blundell, Comparative protein modeling by satisfaction of spatial restraints, J. Mol. Biol. 234 (1993) 779–815.
[19] E.F. Pettersen, T.D. Goddard, C.C. Huang, G.S. Couch, D.M. Greenblatt, E.C. Meng, et al., UCSF Chimera-a visualization system for exploratory research and analysis, J. Comput. Chem. 25 (13) (2004) 1605–1612.
[20] F. Nejatollahi, S.J. Hodgetts, P.J. Vallely, J.P. Burnie, Neutralising human recombinant antibodies to human cytomegalovirus glycoproteins gB and gH, FEMS Immunol. Med. Microbiol. 34 (3) (2002) 237–244.
[21] F. Nejatollahi, Z. Malek-Hosseini, D. Mehrabani, Development of single chain antibodies to P185 tumor antigen, Iran Red Crescent Med J 10 (4) (2008) 298–302.
[22] Marco Biasini, Stefan Bienert, Andrew Waterhouse, Konstantin Arnold, Gabriel Studer, Tobias Schmidt, Florian Kiefer, Tiziano Gallo Cassarino, Martino Bertoni, Lorenza Bordoli, Torsten Schwede, SWISS-MODEL: modeling protein tertiary and quaternary structure using evolutionary information, Nucleic Acids Res. 42 (2014) W252–W258.
[23] L. Bordoli, F. Kiefer, K. Arnold, P. Benkert, J. Battey, T. Schwede, Protein structure homology modeling using SWISS-MODEL Workspace, Nat. Protoc. 4 (1) (2009).
[24] K.B.L. Arnold, J. Kopp, T. Schwede, The SWISS-MODEL Workspace: a web-based environment for protein structure homology modeling, Bioinformatics 22 (2006) 195–201.
[25] J.T. Wei, Urinary biomarkers for prostate cancer, Curr. Opin. Urol. 25 (1) (2015) 77–82.
[26] S. McGrath, D. Christidis, M. Perera, S.K. Hong, T. Manning, I. Vela, et al., Prostate cancer biomarkers: are we hitting the mark? Prostate Int. 4 (4) (2016) 130–135.
[27] M. Mohammadi, F. Nejatollahi, 3D structural modeling of neutralizing SCFV against glycoprotein-D of HSV-1 and evaluation of antigen-antibody interactions by bioinformatic methods, Int. J. Pharm. Bio Sci. 5 (4) (2014) 835–847 (B).
[28] M. Mohammadi, F. Nejatollahi, A. Sakhteman, N. Zarei, Insilico analysis of three different tag polypeptides with dual roles in scFv antibodies, J. Theor. Biol. 402 (2016) 100–106.
[29] M.P. Gibson, Q. Liu, Q. Zhu, Y. Lu, P. Jani, X. Wang, et al., Role of the NH_2-terminal fragment of dentin sialophosphoprotein in dentinogenesis, Eur. J. Oral Sci. 121 (2) (2013) 76–85.
[30] F. Hosseinzadeh, S. Mohammadi, F. Nejatollahi, Production and evaluation of specific single-chain antibodies against CTLA-4 for cancer-targeted therapy, Rep. Biochem. Mol. Biol. 6 (1) (2017) 8–14.
[31] S.S. Mohammadi, F. Hosseinzadeh, F. Nejatollahi, Production of specific anti-EGFR single chain antibodies: a promising strategy in the immunotherapy of EGFR expressing tumor tissues, Int. J. Cancer Manag. 10 (1) (2017).
[32] M. Zemlin, M. Klinger, J. Link, C. Zemlin, K. Bauer, J.A. Engler, et al., Expressed murine and human CDR-H3 intervals of equal length exhibit distinct repertoires that differ in their amino acid composition and predicted range of structures, J. Mol. Biol. 334 (4) (2003) 733–749.
[33] E.A. Kabat, T.T. Wu, Identical V region amino acid sequences and segments of sequences in antibodies of different specificities. Relative contributions of VH and VL genes, minigenes, and complementarity-determining regions to binding of antibody-combining sites, J. Immunol. (Baltimore, Md: 1950) 147 (5) (1991) 1709–1719.
[34] J. Li, Y. Wang, Z. Wang, Z. Dong, Influences of amino acid sequences in FR1 region on binding activity of the scFv and Fab of an antibody to human gastric cancer cells, Immunol. Lett. 71 (3) (2000) 157–165.
[35] M.B. Khalifa, M. Weidenhaupt, L. Choulier, J. Chatellier, N. Rauffer-Bruyere, D. Altschuh, et al., Effects on interaction kinetics of mutations at the VH-VL interface of Fabs depend on the structural context, J. Mol. Recog. 13 (3) (2000) 127–139.
[36] L. Xin, H. Yu, Q. Hong, X. Bi, X. Zhang, Z. Zhang, et al., Identification of strategic residues at the interface of antigen-antibody interactions by in silico mutagenesis, Interdiscip. Sci. Comput. Life Sci. 17 (0242–7) (2017) 1–11.
[37] I. Sela-Culang, V. Kunik, Y. Ofran, The structural basis of antibody-antigen recognition, Front. Immunol. 4 (2013) 302.
[38] J.P. Gallivan, D.A. Dougherty, Cation-pi interactions in structural biology, Proc. Natl. Acad. Sci. U. S. A. 96 (17) (1999) 9459–9464.
[39] R. Reverberi, L. Reverberi, Factors affecting the antigen-antibody reaction, Blood transfusion = Trasfusione del sangue. 5 (4) (2007) 227–240.
[40] T. Nakayama, E. Mizohata, T. Yamashita, S. Nagatoishi, M. Nakakido, H. Iwanari, et al., Structural features of interfacial tyrosine residue in ROBO1 fibronectin domain-antibody complex: crystallographic, thermodynamic, and molecular dynamic analyses, Protein Sci. Publ. Protein Soc. 24 (3) (2015) 328–340.
[41] T. Ramaraj, T. Angel, E.A. Dratz, A.J. Jesaitis, B. Mumey, Antigen-antibody interface properties: composition, residue interactions, and features of 53 non-redundant structures, Biochim. Biophys. Acta 1824 (3) (2012) 520–532.
[42] W. Zheng, J. Ruan, G. Hu, K. Wang, M. Hanlon, J. Gao, Analysis of conformational B-cell epitopes in the antibody-antigen complex using the depth function and the convex hull, PLoS One 10 (8) (2015) e0134835.
[43] L.W. Fisher, A. Jain, M. Tayback, N.S. Fedarko, Small integrin-binding ligand N-linked glycoprotein gene family expression in different cancers, Clin. Cancer Res. 10 (24) (2004) 8501–8511.
[44] C. Wan, G. Yuan, D. Luo, L. Zhang, H. Lin, H. Liu, et al., The dentin sialoprotein (DSP) domain regulates dental mesenchymal cell differentiation through a novel surface receptor, Sci. Rep. 6 (2016) 29666.